

NEW CARRÉ EQUATION

Pedro Americo Almeida Magalhaes Junior, Perrin Smith Neto, Cristina Almeida Magalhães

Pontifícia Universidade Católica de Minas Gerais, Av. Dom Jose Gaspar 500, CEP 30535-610, Belo Horizonte, Minas Gerais, Brazil
(✉ paamj@oi.com.br, +55 31 3221 6813, psmith@pucminas.br, crisamagalhaes@hotmail.com)

Abstract

The present work offers new equations for phase evaluation in measurements. Several phase-shifting equations with an arbitrary but constant phase-shift between captured intensity signs are proposed. The equations are similarly derived as the so called Carré equation. The idea is to develop a generalization of the Carré equation that is not restricted to four images. Errors and random noise in the images cannot be eliminated, but the uncertainty due to their effects can be reduced by increasing the number of observations. An experimental analysis of the errors of the technique was made, as well as a detailed analysis of errors of the measurement. The advantages of the proposed equation are its precision in the measures taken, speed of processing and the immunity to noise in signs and images.

Keywords: metrology, Moiré techniques, fringe analysis, phase measurement, phase shifting technique, Carré equation.

© 2010 Polish Academy of Sciences. All rights reserved

1. Introduction

Phase shifting is an important technique in experimental mechanics [1–3]. Conventional phase shifting equations require phase shift amounts to be known; however, errors in phase shifts are common for the phase shift modulators in real applications, and such errors can further cause substantial errors in the determination of phase distributions. There are many potential error sources which may affect the accuracy of the practical measurement, *e.g.* the phase shifting errors, detector nonlinearities, quantization errors, source stability, vibrations and air turbulence, and so on [4].

Currently, the phase shifting technique is the most widely used technique for evaluation of interference fields in many areas of science and engineering. Its principle is based on the evaluation of the phase values from several phase modulated measurements of the intensity of the interference field. It is necessary to carry out at least three phase-shifted intensity measurements to determine the phase unambiguously and very accurately, at every point of the detector plane. The phase shifting technique offers fully automatic calculation of the phase difference between two coherent wave fields that interfere in the process. There are various phase shifting equations for phase calculation that differ on the number of phase steps, on phase shift values between captured intensity frames, and on their sensitivity to the influencing factors during practical measurements [4].

The general principle of most interferometric measurements is as follows. Two light beams (reference and object) interfere after an interaction of the object beam with the measured object, *i.e.* the beam is transmitted or reflected by the object. The distribution of the intensity of the interference field is then detected, *e.g.* using a photographic film, CCD camera. The phase difference between the reference and the object beam can be determined using the mentioned phase calculation technique. The phase shifting technique is based on an

evaluation of the phase of the interference signal using phase modulation of this interference signal [5].

2. Theory of phase shifting technique

The fringe pattern is assumed to be a sinusoidal function and it is represented by intensity distribution $I(x, y)$. This function can be written in general form as:

$$I(x, y) = I_m(x, y) + I_a(x, y) \cos[\varphi(x, y) + \delta], \quad (1)$$

where I_m is the background intensity variation, I_a is the modulation strength, $\varphi(x, y)$ is the phase at origin and δ is the phase shift related to the origin [6].

The general theory of synchronous detection can be applied to discrete sampling procedure, with only a few sample points. There must be at least four signal measurements needed to determine the phase φ and the term δ . Phase Shifting is the preferred technique whenever the external turbulence and mechanical conditions of the images remain constant over the time required to obtain the four phase-shifted frames. Typically, the technique used in this experiment is called Carré equation [7]. By solving Eq. (1), the phase φ can be determined. The intensity distribution of fringe pattern in a pixel may be represented by gray level, which varies from 0 to 255. With Carré equation, the phase shift (δ) is treated as an unknown parameter. The equation uses four phase-shifted images expressed as:

$$\begin{cases} I_1(x, y) = I_m(x, y) + I_a(x, y) \cos\left[\varphi(x, y) - \frac{3\delta}{2}\right] \\ I_2(x, y) = I_m(x, y) + I_a(x, y) \cos\left[\varphi(x, y) - \frac{\delta}{2}\right] \\ I_3(x, y) = I_m(x, y) + I_a(x, y) \cos\left[\varphi(x, y) + \frac{\delta}{2}\right] \\ I_4(x, y) = I_m(x, y) + I_a(x, y) \cos\left[\varphi(x, y) + \frac{3\delta}{2}\right] \end{cases} \quad (2)$$

Assuming the phase shift is linear and does not change during the measurements, the phase at each point is determined:

$$\varphi = \arctan\left\{\frac{\sqrt{[(I_1 - I_4) + (I_2 - I_3)] [3(I_2 - I_3) - (I_1 - I_4)]}}{(I_2 + I_3) - (I_1 + I_4)}\right\}. \quad (3)$$

Expanding Eq. (3), we obtain the Carré equation:

$$\tan(\varphi) = \frac{\sqrt{\begin{vmatrix} -I_1^2 & +2I_1I_2 & -2I_1I_3 & +2I_1I_4 \\ & +3I_2^2 & -6I_2I_3 & -2I_2I_4 \\ & & +3I_3^2 & +2I_3I_4 \\ & & & -I_4^2 \end{vmatrix}}}{|-I_1 + I_2 + I_3 - I_4|} \quad (4)$$

or emphasizing only the matrix of coefficients of the numerator and the denominator:

$$\tan(\phi) = \frac{\sqrt{\sum_{r=1}^4 \sum_{s=r}^4 n_{r,s} I_r I_s}}{\left| \sum_{r=1}^4 d_r I_r \right|} \left\{ \begin{array}{l} Num = \begin{bmatrix} n_{1,1} & n_{1,2} & n_{1,3} & n_{1,4} \\ & n_{2,2} & n_{2,3} & n_{2,4} \\ & & n_{3,3} & n_{3,4} \\ & & & n_{4,4} \end{bmatrix}, \quad Dem = [d_1 \quad d_2 \quad d_3 \quad d_4] \\ Num = \begin{bmatrix} -1 & 2 & -2 & 2 \\ & 3 & -6 & -2 \\ & & 3 & 2 \\ & & & -1 \end{bmatrix}, \quad Dem = [-1 \quad 1 \quad 1 \quad -1] \end{array} \right. \quad (5)$$

Almost all the existing phase-shifting equations are based on the assumption that the phase-shift at all pixels of the intensity frame is equal and known. However, it may be very difficult to achieve this in practice. Phase measuring equations are more or less sensitive to some types of errors that can occur during measurements with images. The phase-shift value is assumed to be unknown but constant in phase calculation equations, which are derived in this article. Consider now the constant but unknown phase shift δ between recorded images of the intensity of the observed interference field.

Considering N phase-shifted intensity measurements, we can write for the intensity distribution I_k at every point of k recorded phase-shifted interference patterns.

$$I_k(x, y) = I_m(x, y) + I_a(x, y) \cos \left[\varphi(x, y) + \left(\frac{2k - N - 1}{2} \right) \delta \right], \quad (6)$$

where $k = 1, \dots, N$ and N is the number of frames.

In Novak [4], several five-step phase-shifting equations insensitive to phase shift calibration are described and a complex error analysis of these phase calculation equations is performed. The best five-step equation, Eq. (7), seems to be a very accurate and stable phase-shifting equation with the unknown phase step for a wide range of phase step values.

$$\begin{cases} a_{jk} = I_j - I_k \\ b_{jk} = I_j + I_k \end{cases} \quad \tan(\phi) = \frac{\sqrt{4a_{24}^2 - a_{15}^2}}{2I_3 - b_{15}} = \frac{\sqrt{4(I_2 - I_4)^2 - (I_1 - I_5)^2}}{2I_3 - I_1 - I_5}. \quad (7)$$

Expanding Eq. (7), we obtain the Novak equation:

$$\tan(\phi) = \frac{\sqrt{\begin{vmatrix} -I_1^2 & & & +2I_1I_5 \\ & +4I_2^2 & & -8I_2I_4 \\ & & & +4I_4^2 \\ & & & & -I_5^2 \end{vmatrix}}}{|-I_1 + 2I_3 - I_5|} \quad (8)$$

or emphasizing only the matrix of coefficients of the numerator and the denominator:

$$\tan(\phi) = \frac{\sqrt{\sum_{r=1}^5 \sum_{s=r}^5 n_{r,s} I_r I_s}}{\left| \sum_{r=1}^5 d_r I_r \right|} \left\{ \begin{array}{l} \text{Num} = \begin{bmatrix} n_{1,1} & n_{1,2} & n_{1,3} & n_{1,4} & n_{1,5} \\ & n_{2,2} & n_{2,3} & n_{2,4} & n_{2,5} \\ & & n_{3,3} & n_{3,4} & n_{3,5} \\ & & & n_{4,4} & n_{4,5} \\ & & & & n_{5,5} \end{bmatrix}, \text{Dem} = [d_1 \ d_2 \ d_3 \ d_4 \ d_5] \\ \text{Num} = \begin{bmatrix} -1 & 0 & 0 & 0 & 2 \\ & 4 & 0 & -8 & 0 \\ & & 0 & 0 & 0 \\ & & & 4 & 0 \\ & & & & -1 \end{bmatrix}, \text{Dem} = [-1 \ 0 \ 2 \ 0 \ -1] \end{array} \right. \quad (9)$$

3. Uncertainty analysis

Following the model of uncertainty analysis presented in [8], these new equations have excellent results with the application of Monte Carlo-based technique of uncertainty propagation. The Monte Carlo-based technique requires assigning probability density functions (PDFs) to each input quantity. A computer algorithm is set up to generate an input vector $P = (p_1 \dots p_n)^T$; each element p_j of this vector is generated according to the specific PDF assigned to the corresponding quantity p_j . By applying the generated vector P to the model $Q = M(P)$, the corresponding output value Q can be computed. If the simulating process is repeated n times ($n \gg 1$), the outcome is a series of indications ($q_1 \dots q_n$) whose frequency distribution allows us to identify the PDF of Q . Then, irrespective of the form of this PDF, the estimate q_e and its associated standard uncertainty $u(q_e)$ can be calculated by:

$$q_e = \frac{1}{n} \sum_{l=1}^n q_l, \quad (10)$$

and

$$u(q_e) = \sqrt{\frac{1}{(n-1)} \sum_{l=1}^n (q_l - q_e)^2}. \quad (11)$$

The influence of the error sources affecting the phase values is considered in these models through the values of the intensity I_k . This is done by modifying Eq. (6):

$$I_k(x, y) = I_m(x, y) + I_a(x, y) \cos \left[\phi(x, y) + \left(\frac{2k - N - 1}{2} \right) (\delta + \theta) + \varepsilon_k \right] + \xi_k. \quad (12)$$

Comparing Eqs. (6) and (12), it can be observed that three input quantities (θ , ε_k , ξ_k) were included. θ allows us to consider in the uncertainty propagation the systematic error used to induce the phase shift, is not adequately calibrated. The error bound allowed us to assign to θ a rectangular PDF over the interval $[-\pi/10 \text{ rad}, +\pi/10 \text{ rad}]$. ε_k allows us to account for the influence of environmental perturbations. The error bound allowed us to assign to ε_k a rectangular PDF over the interval $[-\pi/20 \text{ rad}, +\pi/20 \text{ rad}]$. ξ_k allows us to account for the nearly random effect of the optical noise [8]. The rectangular PDFs assigned to ξ_k should be in the interval $[-10, +10]$.

The values of ϕ were considered given in the range $[0, \pi/2]$. A computer algorithm was set up to generate single values of (θ , ε_k , ξ_k) according to the corresponding PDFs. With the generated values of the input quantities, we evaluated the phase ϕ' by using the new equations. Since this simulating process and the corresponding phase evaluation were

repeated $n = 10^4 = 10000$ times, we were able to form the series $(\phi'_1 \dots \phi'_{10000})$ with the outcomes [8].

4. Proposed equations

Here is proposed a general equation for calculating the phase for any number, N , of images where:

$$\tan(\phi) = \frac{\sqrt{\sum_{r=1}^N \sum_{s=r}^N n_{r,s} I_r I_s}}{\left| \sum_{r=1}^N d_r I_r \right|}, \tag{13}$$

where N is the number of images, $n_{r,s}$ are coefficients of the numerator, d_r are coefficients of the denominator, r and s are indexes of the sum. Or, expanding the summations and allowing an arbitrary number of lines obtains:

$$\tan(\phi) = \frac{\sqrt{\begin{matrix} n_{1,1}I_1^2 & + n_{1,2}I_1I_2 & + n_{1,3}I_1I_3 & + n_{1,4}I_1I_4 & \dots & + n_{1,N}I_1I_N \\ & + n_{2,2}I_2^2 & + n_{2,3}I_2I_3 & + n_{2,4}I_2I_4 & \dots & + n_{2,N}I_2I_N \\ & & + n_{3,3}I_3^2 & + n_{3,4}I_3I_4 & \dots & + n_{3,N}I_3I_N \\ & & & + n_{4,4}I_4^2 & \dots & + n_{4,N}I_4I_N \\ & & & & \dots & \dots \\ & & & & & + n_{N,N}I_N^2 \end{matrix}}{|d_1I_1 + d_2I_2 + d_3I_3 + d_4I_4 + \dots + d_{N-1}I_{N-1} + d_NI_N|}. \tag{14}$$

Emphasizing only the matrix of coefficients of the numerator and the denominator:

$$\tan(\phi) = \frac{\sqrt{\sum_{r=1}^N \sum_{s=r}^N n_{r,s} I_r I_s}}{\left| \sum_{r=1}^N d_r I_r \right|} \left\{ \begin{array}{l} Num = \begin{bmatrix} n_{1,1} & n_{1,2} & n_{1,3} & n_{1,4} & \dots & n_{1,N} \\ & n_{2,2} & n_{2,3} & n_{2,4} & \dots & n_{2,N} \\ & & n_{3,3} & n_{3,4} & \dots & n_{3,N} \\ & & & n_{4,4} & \dots & n_{4,N} \\ & & & & \dots & \dots \\ & & & & & n_{N,N} \end{bmatrix} \\ Dem = [d_1 \quad d_2 \quad d_3 \quad d_4 \quad \dots \quad d_{N-1} \quad d_N] \end{array} \right. \tag{15}$$

The display of the phase calculation equation in this way permits the viewing of symmetries and plans of sparse matrix. The use of the absolute value in the numerator and the denominator restricts the angle between 0 and $\pi/2$ rad, but avoids negative roots and also eliminates finding false angles. Subsequent considerations will later remove this restriction [4–6].

In the tested practical applications, an increase of 20% in processing time was noticed when using 16 images instead of 4, while processing the standard Carré equation, due to many zero coefficients. But if one changes the coefficients from integer type to real numbers, the processing time for the evaluation of phase is almost doubled, because real numbers require more memory and more processing time to evaluate floating point additions and multiplications, which are many in the equations with large number of images.

The shift on the problem focus of obtaining equations for calculating the phase of an analytical problem of a numerical vision is a great innovation. It breaks a paradigm that was hitherto used by several authors. After several attempts in numerical modeling of the problem, the following mathematical problem was identified (16, 17, 18, 19):

$$\text{Minimal } \sqrt{\frac{\sum_{\tau=1}^n (\phi_*^\tau - \bar{\phi}_*)^2}{n-1}} \quad \text{where } \bar{\phi}_* = \frac{\left(\sum_{\tau=1}^n \phi_*^\tau\right)}{n} \quad \text{and } n = 10000 \quad (16)$$

$$\text{subject } \left\{ \begin{array}{ll} \text{i)} \quad \tan^2(\phi^v) \left(\sum_{r=1}^N d_r I_r^v \right)^2 = \sum_{r=1}^N \sum_{s=r}^N n_{r,s} I_r^v I_s^v, & \begin{array}{l} \text{number of variables}(v) \\ v = 1.. \left[\frac{(N+1)N}{2} + N \right] \end{array} \\ \text{ii)} \quad \sum_{s=r}^N |n_{r,s}| + |d_r| \geq 1, & r = 1..N, \text{enter all frames} \\ \text{iii)} \quad \sum_{s=r}^N |n_{s,r}| + |d_r| \geq 1, & r = 1..N, \text{enter all frames} \\ \text{iv)} \quad -2N \leq n_{r,s} \leq 2N, & r = 1..N, s = r..N \\ \text{v)} \quad -2N \leq d_r \leq 2N, & r = 1..N \\ \text{vi)} \quad n_{r,s} \text{ are integer,} & r = 1..N, s = r..N \\ \text{vii)} \quad d_r \text{ are integer,} & r = 1..N \\ \text{viii)} \quad \phi_*^\tau = \arctan \left(\frac{\sqrt{\sum_{r=1}^N \sum_{s=r}^N n_{r,s} \hat{I}_r^\tau \hat{I}_s^\tau}}{\sum_{r=1}^N d_r \hat{I}_r^\tau} \right) & \tau = 1..n \end{array} \right. \quad (17)$$

where for each v :

$$\left\{ \begin{array}{l} I_k^v(x, y) = I_m^v(x, y) + I_a^v(x, y) \cos \left[\varphi^v(x, y) + \left(\frac{2k - N - 1}{2} \right) \delta^v \right], k = 1..N \\ I_m^v \in [0; 128] \quad \text{random and real} \\ I_a^v \in [0; 127] \quad \text{random and real} \\ \varphi^v \in [-\pi; \pi] \quad \text{random and real} \\ \delta^v \in [-2\pi; 2\pi] \quad \text{random and real} \end{array} \right. \quad (18)$$

where for each r :

$$\left\{ \begin{array}{l}
 \hat{I}_k^\tau(x, y) = \hat{I}_m^\tau(x, y) + \hat{I}_a^\tau(x, y) \cos \left[\hat{\phi}^\tau(x, y) + \left(\frac{2k - N - 1}{2} \right) (\hat{\delta}^\tau + \hat{\theta}^\tau) + \hat{\varepsilon}_k^\tau \right] + \hat{\xi}_k^\tau \\
 \text{com} \quad k = 1..N \\
 \hat{I}_m^\tau \in [0; 128] \quad \text{random and real} \\
 \hat{I}_a^\tau \in [0; 127] \quad \text{random and real} \\
 \hat{\phi}^\tau \in [0; \pi/2] \quad \text{random and real} \\
 \hat{\delta}^\tau \in [-2\pi; 2\pi] \quad \text{random and real} \\
 \hat{\theta}^\tau \in [-\pi/20; \pi/20] \quad \text{random and real} \\
 \hat{\varepsilon}_k^\tau \in [-\pi/10; \pi/10] \quad \text{random and real} \\
 \hat{\xi}_k^\tau \in [-10; 10] \quad \text{random and real}
 \end{array} \right. \quad (19)$$

The coefficients of the matrices of the numerator ($n_{r,s}$) and the denominator (d_r) must be integers to increase the performance of the computer algorithm, as the values of the intensity of the images (I_k) are also integers ranging from 0 to 255. Modern computers perform integer computations (additions and multiplications) much faster than floating point ones. It should be noted that the modern commercial digital cameras already present graphics resolution above 12 Mega pixels and that the evaluation of phase (ϕ) should be done pixel by pixel. Another motivation is the memory usage: integer values can be represented by a single byte while real values use at least 4 bytes. The present scheme uses real numbers only in the square root of the numerator, in the division by denominator and in the arc-tangent over the entire operation.

The idea is to obtain the values of the coefficients of matrices of the numerator ($n_{r,s}$) and denominator (d_r) with the minimum standard uncertainty the phase values $u(\phi)$ in Eq. (11). It comes from the attempt to force these factors to zero, for computational speed-up and for reducing the amount of the memory required, since zero terms in sparse matrices do not need to be stored. It is also important that those ratios are not very large so that the sum of the numerator and the denominator does not have a very high value to fit into an integer variable. For a precise phase evaluation, these factors will increase the values of the intensity of the image (I_k) that contains errors due to noise in the image, in its discretization in pixels and in shades of gray.

The first restriction of the problem (16, 17, 18, 19) is the Eq. (13), which is squared to form the relation that one is seeking. It should be noted that the results obtained by solving the mathematical problem of the coefficients are in the form of matrices for the numerator ($n_{r,s}$) and the denominator (d_r), so the number of unknowns is given by ν . To ensure that one has a hyper-restricted problem, the number of restrictions must be greater than or at least equal to the number of variables. The ν restrictions of the model are obtained through random choice of values for I_m , I_a , ϕ and δ and by using the Eq. (6) to compute I_k . Tests showed that even for low numbers for other values of ν , the mathematical problem leads to only one optimal solution though it becomes more time-consuming. Indeed the values of I_m , I_a , ϕ and δ can be any real number, but to maintain compatibility with the problem images, it was decided to limit I_m between 0 to 128 and I_a between 0 and 127 so that I_k would be between 0 and 255.

The restrictions *ii* and *iii* of the problem are based on the idea that all image luminous intensities, I_k , must be present in the equation. It increases the amounts of samples to reduce the noise of random images. This requires that all of the sampling images enter the equation for phase calculation. This is achieved by imposing that the sum of the absolute values of the

Restrictions iv and v of the problem are used to accelerate the solution of this mathematical model. This limitation in the value of the coefficients of matrices of the numerator ($n_{r,s}$) and denominator (d_r) presents a significant reduction in the search universe and in the search of a solution for model optimization. Restriction $viii$ of the problem (16, 17, 18, 19) is the Eq. (12).

The following multi-step equation for phase calculation uses well known trigonometric relations and branch-and-bound algorithm [9] for pure integer nonlinear programming with the mathematic problem (16, 17, 18, 19). Table 1 shows equations.

5. Tests of uncertainty analysis

The objectives are equations of phase calculation, better, more accurate, more robust and more stable for the random noise. The tests show that the optimum phase-shift interval with which the equation gives minimum uncertainty for the noise is in the vicinity of $\pi/2$ rad (Fig. 1).

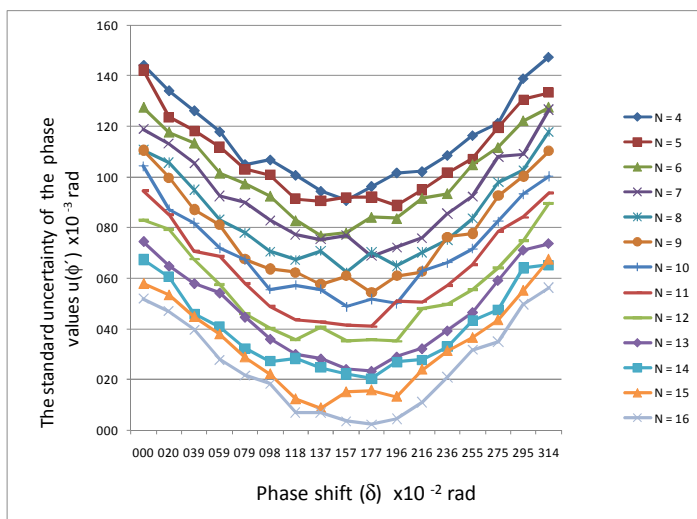


Fig. 1. Standard uncertainty of the phase values $u(\phi)$ using new equations with variation of phase shift (δ). Note that the uncertainty is smaller near $\delta = \pi/2$ radian and decreases with increasing number of images.

Fig. 2 shows the relationship between the standard uncertainty and the phase values ϕ in the range $[-\pi, \pi]$. This relationship expresses the accuracy and stability of the proposed phase shifting equations. Further, there were studied the properties of the equations with respect to the change of parameters simulating the real nonlinearities of the phase shifting device and detector.

Fig. 3 shows the average of the standard uncertainty $u(\phi)$ generated with values ϕ in the range $[0, \pi/2]$ by using new equations. It can be observed that the uncertainty by new equations diminishes as the number of images increases.

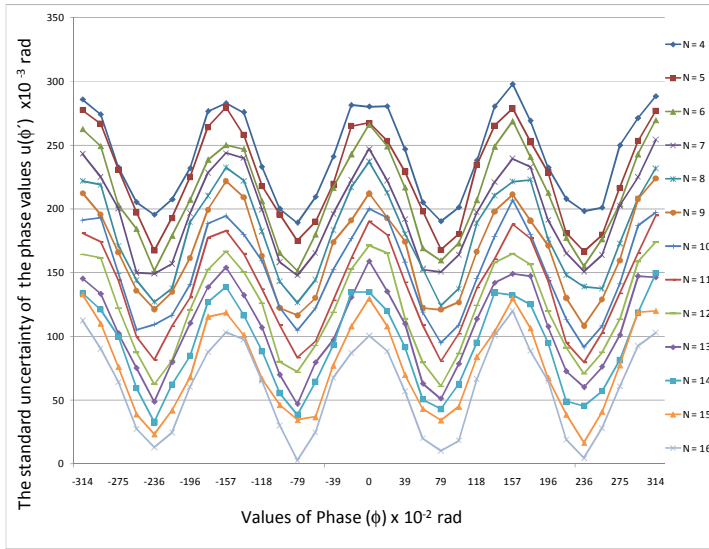


Fig. 2. Standard uncertainty of the phase values $u(\phi')$ using new equations with variation of phase (ϕ) . Note that the uncertainty is smaller near the multiples of $\phi = \pi/4$ radian and decreases with an increasing number of images.

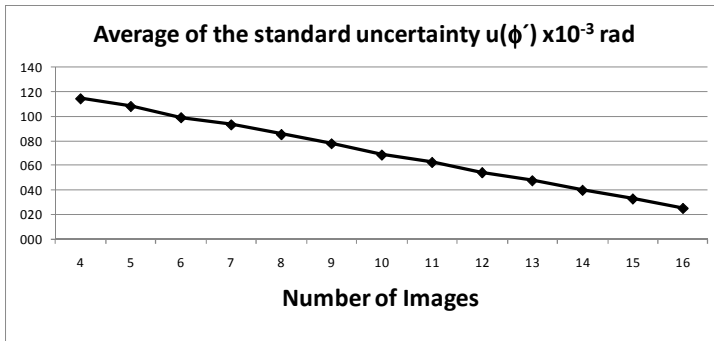


Fig. 3. Average of the standard uncertainty $u(\phi')$ by using new equations. Note that the uncertainty decreases with an increasing number of images.

6. Symmetry and sparse matrix of coefficients

To solve the problem of increasing the processing time to obtain new equations for phase calculation with the increased number of variables for high values of N uses up an important data; the equations showed symmetries in the matrix of coefficients of numerator and the denominator (Fig. 4). Let $h = (N \text{ div } 2) + (N \text{ mod } 2)$, where the value of $x \text{ div } y$ is the value of x/y down rounded to the nearest integer (integer division) and the mod operator returns the remainder obtained by dividing its operands (in other words, $x \text{ mod } y = x - (x \text{ div } y) * y$). The symmetries are:

$$\left\{ \begin{array}{ll} d_r = d_{N+1-r}, & r = 1..h \text{ and } r \neq N+1-r \\ n_{r,N+1-r} = -2n_{r,r}, & r = 1..h \text{ and } r \neq N+1-r \\ n_{N+1-s,N+1-r} = n_{r,s}, & r = 1..h; s = r..h \text{ and } r \neq N+1-s \text{ and } s \neq N+1-r \\ n_{r,N+1-s} = -n_{r,s}, & r = 1..h; s = r..h \text{ and } s > r \text{ and } s \neq N+1-r \\ n_{s,N+1-r} = -n_{r,s}, & r = 1..h; s = r..h \text{ and } s > r \text{ and } s \neq N+1-r \end{array} \right. \quad (20)$$

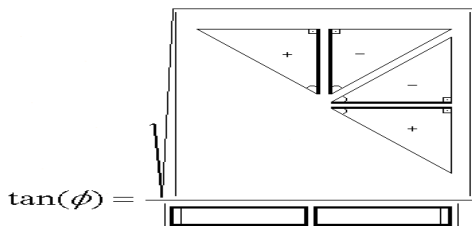


Fig. 4. Symmetries in the coefficients of the numerator and denominator.

So as the matrix for N also was:

$$\text{Num} = \begin{bmatrix} n_{1,1} & n_{1,2} & n_{1,3} & \dots & n_{1,h-1} & n_{1,h} & -n_{1,h} & -n_{1,h-1} & \dots & -n_{1,3} & -n_{1,2} & -2n_{1,1} \\ & n_{2,2} & n_{2,3} & \dots & n_{2,h-1} & n_{2,h} & -n_{2,h} & -n_{2,h-1} & \dots & -n_{2,3} & -2n_{2,2} & -n_{1,2} \\ & & n_{3,3} & \dots & n_{3,h-1} & n_{3,h} & -n_{3,h} & -n_{3,h-1} & \dots & -2n_{3,3} & -n_{2,3} & -n_{1,3} \\ & & & \dots \\ & & & & n_{h-1,h-1} & n_{h-1,h} & -n_{h-1,h} & -2n_{h-1,h-1} & \dots & -n_{3,h-1} & -n_{2,h-1} & -n_{1,h-1} \\ & & & & & n_{h,h} & -2n_{h,h} & -n_{h-1,h} & \dots & -n_{3,h} & -n_{2,h} & -n_{1,h} \\ & & & & & & n_{h,h} & n_{h-1,h} & \dots & n_{3,h} & n_{2,h} & n_{1,h} \\ & & & & & & & n_{h-1,h-1} & \dots & n_{3,h-1} & n_{2,h-1} & n_{1,h-1} \\ & & & & & & & & \dots & \dots & \dots & \dots \\ & & & & & & & & & n_{3,3} & n_{2,3} & n_{1,3} \\ & & & & & & & & & & n_{2,2} & n_{1,2} \\ & & & & & & & & & & & n_{1,1} \end{bmatrix} \quad (21)$$

$$\text{Dem} = [d_1 \ d_2 \ d_3 \ d_4 \ \dots \ d_{h-1} \ d_h \ d_h \ d_{h-1} \ \dots \ d_4 \ d_3 \ d_2 \ d_1]$$

As well the matrix for odd N was:

$$\text{Num} = \begin{bmatrix} n_{1,1} & n_{1,2} & n_{1,3} & \dots & n_{1,h-1} & n_{1,h} & -n_{1,h-1} & \dots & -n_{1,3} & -n_{1,2} & -2n_{1,1} \\ & n_{2,2} & n_{2,3} & \dots & n_{2,h-1} & n_{2,h} & -n_{2,h-1} & \dots & -n_{2,3} & -2n_{2,2} & -n_{1,2} \\ & & n_{3,3} & \dots & n_{3,h-1} & n_{3,h} & -n_{3,h-1} & \dots & -2n_{3,3} & -n_{2,3} & -n_{1,3} \\ & & & \dots \\ & & & & n_{h-1,h-1} & n_{h-1,h} & -2n_{h-1,h-1} & \dots & -n_{3,h-1} & -n_{2,h-1} & -n_{1,h-1} \\ & & & & & n_{h,h} & n_{h-1,h} & \dots & n_{3,h} & n_{2,h} & n_{1,h} \\ & & & & & & n_{h-1,h-1} & \dots & n_{3,h-1} & n_{2,h-1} & n_{1,h-1} \\ & & & & & & & \dots & \dots & \dots & \dots \\ & & & & & & & & n_{3,3} & n_{2,3} & n_{1,3} \\ & & & & & & & & & n_{2,2} & n_{1,2} \\ & & & & & & & & & & n_{1,1} \end{bmatrix} \quad (22)$$

$$\text{Dem} = [d_1 \ d_2 \ d_3 \ d_4 \ \dots \ d_{h-1} \ d_h \ d_{h-1} \ \dots \ d_4 \ d_3 \ d_2 \ d_1]$$

Therefore, using symmetry to the numerator coefficients can be represented with only its first quarter and the denominator coefficients can be represented only with the first half, as shown below:

$$Num^{1/4} = \begin{bmatrix} n_{1,1} & n_{1,2} & n_{1,3} & \dots & n_{1,h-1} & n_{1,h} \\ & n_{2,2} & n_{2,3} & \dots & n_{2,h-1} & n_{2,h} \\ & & n_{3,3} & \dots & n_{3,h-1} & n_{3,h} \\ & & & \dots & \dots & \dots \\ & & & & n_{h-1,h-1} & n_{h-1,h} \\ & & & & & n_{h,h} \end{bmatrix} \quad Dem^{1/2} = [d_1 \ d_2 \ d_3 \ \dots \ d_{h-1} \ d_h] \quad (23)$$

In the previous equations (23), most of the coefficients of the numerator and the denominator are zero. And even more for the first quarter of the coefficients of the numerator, the terms are different from zero in the main diagonal and closer to the three diagonals, so only the first four coefficients of each line are different from zero. In the first half of the coefficients of the denominator, only the first four and the last term are different from zero. A matrix where most of the terms are zeros is usually called sparse matrix.

$$\text{Sparse} \quad \begin{cases} d_r^{1/2} = 0, & r = 5..h-1 \\ n_{r,s}^{1/4} = 0, & r = 1..h-5, \quad s = r+4..h, \quad \text{and} \quad s > r+3 \end{cases} \quad (24)$$

In order, the matrix is:

$$Num^{1/4} = \begin{bmatrix} n_{1,1} & n_{1,2} & n_{1,3} & n_{1,4} & 0 & 0 & 0 & 0 & 0 & 0 & \dots & 0 \\ & n_{2,2} & n_{2,3} & n_{2,4} & n_{2,5} & 0 & 0 & 0 & 0 & 0 & \dots & 0 \\ & & n_{3,3} & n_{3,4} & n_{3,5} & n_{3,6} & 0 & 0 & 0 & 0 & \dots & 0 \\ & & & n_{4,4} & n_{4,5} & n_{4,6} & n_{4,7} & 0 & 0 & 0 & \dots & 0 \\ & & & & \dots & \dots & \dots & \dots & 0 & 0 & \dots & 0 \\ & & & & & n_{h-6,h-6} & n_{h-6,h-5} & n_{h-6,h-4} & n_{h-6,h-3} & 0 & \dots & 0 \\ & & & & & & n_{h-5,h-5} & n_{h-5,h-4} & n_{h-5,h-3} & n_{h-5,h-2} & 0 & 0 \\ & & & & & & & n_{h-4,h-4} & n_{h-4,h-3} & n_{h-4,h-2} & n_{h-4,h-1} & 0 \\ & & & & & & & & n_{h-3,h-3} & n_{h-3,h-2} & n_{h-3,h-1} & n_{h-3,h} \\ & & & & & & & & & n_{h-2,h-2} & n_{h-2,h-1} & n_{h-2,h} \\ & & & & & & & & & & n_{h-1,h-1} & n_{h-1,h} \\ & & & & & & & & & & & n_{h,h} \end{bmatrix} \quad (25)$$

$$Dem^{1/2} = [d_1 \ d_2 \ d_3 \ d_4 \ 0 \ 0 \ \dots \ 0 \ 0 \ d_h]$$

An important fact is that the resolution of the mathematical model generates new and efficient equations for calculating the phase. As most of the coefficients of both the numerator and the denominator is zero, the implementation of these new equations is very fast and the volume of mathematical operations is reduced, because the terms are zero as there is no need for a multiplier to the values of luminous intensity I_k for these factors, as any number multiplied by zero will be zero.

7. Equations for phase calculation of many images

Analyzing the equations deduced, it was attempted to get a rule for training for them or an algorithm to provide valid values of coefficients of the numerator and the denominator of the equations for phase calculation of large quantities of images ($N > 15$). The concept of

$$\begin{aligned} \text{Half} &= (N + 1)/2 \\ \text{Fourth} &= (N + 1)/4 \end{aligned}$$

$$\begin{aligned} \text{Num}^{1/4} &= \begin{bmatrix} -1 & -2 & 0 & 1 & 0 & \dots \\ & 1 & 1 & -1 & 0 & 0 & \dots \\ & & 0 & 0 & 0 & 0 & \dots \\ & & & 0 & 0 & -1 & 0 & \dots \\ & & & & 1 & 0 & 0 & 0 & \dots \\ & & & & & 0 & 0 & 1 & 0 & \dots \\ & & & & & & -1 & 0 & 0 & 0 & \dots \\ & & & & & & & -1 & 0 & 2 & 0 & \dots \\ & & & & & & & & 0 & 2 & 2 & -2 & 0 & \dots \\ & & & & & & & & & 2 & -2 & 0 & 0 & \dots \\ & & & & & & & & & & 0 & 0 & -1 & 0 & \dots \\ & & & & & & & & & & & 1 & 0 & 0 & \dots \\ & & & & & & & & & & & \dots & \dots & \dots & \dots \\ & & & & & & & & & & & & 0 & 1 & 0 \\ & & & & & & & & & & & & & 1 & 0 \\ & & & & & & & & & & & & & & 0 \end{bmatrix} \begin{array}{l} \text{Row :} \\ 1 \\ 2 \\ 3 \\ 4 \\ 5 \\ \text{Repeat} \\ \text{Repeat} \\ \text{Fourth} - 1 \\ \text{Fourth} \\ \text{Fourth} + 1 \\ \text{Repeat} \\ \text{Repeat} \\ \dots \\ \text{Half} - 2 \\ \text{Half} - 1 \\ \text{Half} \end{array} \end{aligned} \tag{32}$$

$$\begin{aligned} \text{Dem}^{1/2} &= [-1 \quad -1 \quad 1 \quad 0 \quad 0 \quad 0 \quad \dots \quad 0 \quad 0 \quad 2] \\ \text{Col} &: 1 \quad 2 \quad 3 \quad 4 \quad 5 \quad 6 \quad \dots \quad \text{Half} - 2 \quad \text{Half} - 1 \quad \text{Half} \end{aligned}$$

For case 8, when N is odd, $N + 1$ is divisible by 4 but $N + 1$ is not divisible by 8:

$$\begin{aligned} \text{Half} &= (N + 1)/2 \\ \text{Fourth} &= (N + 1)/4 \end{aligned}$$

$$\begin{aligned} \text{Num}^{1/4} &= \begin{bmatrix} -1 & -2 & 0 & 0 & 0 & \dots \\ & 1 & 2 & -1 & 0 & 0 & \dots \\ & & 0 & 0 & -1 & 0 & \dots \\ & & & 1 & 0 & 0 & 0 & \dots \\ & & & & 0 & 0 & 1 & 0 & \dots \\ & & & & & -1 & 0 & 0 & 0 & \dots \\ & & & & & & \dots & \dots & \dots & \dots \\ & & & & & & & -1 & 0 & 2 & 0 & \dots \\ & & & & & & & & 0 & 2 & 2 & -2 & 0 & \dots \\ & & & & & & & & & 2 & -2 & 0 & 0 & \dots \\ & & & & & & & & & & 0 & 0 & -1 & 0 & \dots \\ & & & & & & & & & & & 1 & 0 & 0 & \dots \\ & & & & & & & & & & & \dots & \dots & \dots & \dots \\ & & & & & & & & & & & & 1 & 0 \\ & & & & & & & & & & & & & 0 \end{bmatrix} \begin{array}{l} \text{Row :} \\ 1 \\ 2 \\ 3 \\ 4 \\ \text{Repeat} \\ \text{Repeat} \\ \dots \\ \text{Fourth} - 1 \\ \text{Fourth} \\ \text{Fourth} + 1 \\ \text{Repeat} \\ \text{Repeat} \\ \dots \\ \text{Half} - 1 \\ \text{Half} \end{array} \end{aligned} \tag{33}$$

$$\begin{aligned} \text{Dem}^{1/2} &= [-1 \quad -1 \quad 1 \quad 0 \quad 0 \quad 0 \quad \dots \quad 0 \quad 0 \quad 2] \\ \text{Col} &: 1 \quad 2 \quad 3 \quad 4 \quad 5 \quad 6 \quad \dots \quad \text{Half} - 2 \quad \text{Half} - 1 \quad \text{Half} \end{aligned}$$

As the new equations were developed from the algorithms, numerical calculation, instead of analytical demonstrations of trigonometric relations, is necessary to check them. It is believed that a large number of numerical tests can validate or verify these new equations, or at least reduce to a minimum the chance of these equations being wrong or false. The goal here is to verify that the new equations really calculate the tangent of the phase $\tan(\phi)$. For

that reason, real figures are attributed to random I_m that ranges from 0 to 128 that are assigned at random to real values, I_a that ranges from 0 to 127, and the cosine of -1 varies by 1 to the values of luminous intensity I_k will be between 0 and 255 that is the range of pixel amplitude for a monochrome digital photo. It is interesting to notice that the digital images and values are intact here to further enlarge the test in which they are made real. They are also assigned values to real random ϕ' that varies from $-\pi$ to π , tracking common algorithms used on the main unwrapped. Real values are assigned and the random δ that ranges from -10π to 10π , a very wide range of possible values of step-phase. The values of I_k (image luminosity) are calculated with k ranging from 1 to N . The new equations with the values of I_k are applied, giving a $\tan(\phi)$ that must be compared to the value of phase randomly assigned (ϕ'). This comparison is the accuracy through a very small value because the number of rounding errors that can occur in the calculations, say, precision $|\phi' - \phi| \leq 10^{-6}$. This was done thousands of times (at least 10000 times) for each equation for phase calculation. It generated and made up of at least 99.9% of the time with an accuracy of 10^{-6} . Thus, it was believed that the chances for the equations to be wrong or false have become minimal or remote.

8. Before unwrapping, change $\phi \in [0, \pi/2]$ to $\phi^* \in [-\pi, \pi]$

Because of the character of the evaluation equations, only phase values $\phi \in [0, \pi/2]$ were calculated. For unequivocal determination of the wrapped phase values ϕ it was necessary to test four values $\phi, -\phi, \phi - \pi$ and $-\phi + \pi$ using values of I_k and small systems. With this, the value $\phi^* \in [-\pi, \pi]$ was obtained [3–6]. In case $N=5$, with I_1, I_2, I_3, I_4 and I_5 , δ was found in first equation and the values $\phi, -\phi, \phi - \pi$ and $-\phi + \pi$ were attributed to ϕ^* to test the other equation and I_a was found using a second equation. As an example, for each (x, y) it was tested for the four values $\phi, -\phi, \phi - \pi$ and $-\phi + \pi$ in (Addition and subtraction of first, last and middle frames, the I_k):

$$\text{even } N=4 \left\{ \begin{array}{l} \cos(\delta/2) = \pm \sqrt{\frac{I_1 - I_4}{4(I_2 - I_3)}} \\ I_1 - I_4 = 2I_a \sin(\phi^*) \sin(3\delta/2) \\ I_2 - I_3 = 2I_a \sin(\phi^*) \sin(\delta/2) \\ (I_1 + I_4) - (I_2 + I_3) = 2I_a \cos(\phi^*) [\cos(3\delta/2) - \cos(\delta/2)] \\ I_1 - I_3 = I_a [\cos(\phi^* - 3\delta/2) - \cos(\phi^* + \delta/2)] \end{array} \right. \quad (34)$$

$$\text{odd } N=5 \left\{ \begin{array}{l} \cos(\delta) = \frac{I_1 - I_5}{2(I_2 - I_4)} \\ I_1 - I_5 = 2I_a \sin(\phi^*) \sin(2\delta) \\ I_2 - I_4 = 2I_a \sin(\phi^*) \sin(\delta) \\ I_1 + I_5 - 2I_3 = 2I_a \cos(\phi^*) [\cos(2\delta) - 1] \\ I_2 + I_4 - 2I_3 = 2I_a \cos(\phi^*) [\cos(\delta) - 1] \end{array} \right. \quad (35)$$

In a different approach, for unambiguous determination of the wrapped phase values, it is necessary to test four values $\phi, -\phi, \phi - \pi$ and $-\phi + \pi$ using values of I_k and to solve small nonlinear systems (Newton-Raphson methods). For each angle $\phi, -\phi, \phi - \pi$ and $-\phi + \pi$, solve the nonlinear system by Newton-Raphson in Eq. (36), getting the values of I_m, I_a and δ .

$$\begin{cases} I_1 - \left(I_m + I_a \cos \left[\phi^* + \left(\frac{2.1 - N - 1}{2} \right) \delta \right] \right) = 0 \\ I_2 - \left(I_m + I_a \cos \left[\phi^* + \left(\frac{2.2 - N - 1}{2} \right) \delta \right] \right) = 0 \\ I_3 - \left(I_m + I_a \cos \left[\phi^* + \left(\frac{2.3 - N - 1}{2} \right) \delta \right] \right) = 0 \end{cases} \quad (36)$$

With the values of I_m , I_a and δ , test the Eq. (37) and find the correct angle $\phi^* \in [-\pi, \pi]$.

$$\begin{cases} I_4 - \left(I_m + I_a \cos \left[\phi^* + \left(\frac{2.4 - N - 1}{2} \right) \delta \right] \right) = 0 \\ \dots \\ I_N - \left(I_m + I_a \cos \left[\phi^* + \left(\frac{2N - N - 1}{2} \right) \delta \right] \right) = 0 \end{cases} \quad (37)$$

9. Testing and analysis of error

The phase ϕ^* obtained from the phase shifting algorithm above is a wrapped phase which varies from $-\pi/2$ to $\pi/2$. The relationship between the wrapped phase and the unwrapped phase may thus be stated as:

$$\Psi(x, y) = \phi^*(x, y) + 2\pi j(x, y), \quad (38)$$

where j is an integer number, ϕ^* is a wrapped phase and Ψ is an unwrapped phase.

The next step is to unwrap the wrapped phase map. When unwrapping, several of the phase values should be shifted by an integer multiple of 2π . Unwrapping is thus adding or subtracting 2π offsets at each discontinuity encountered in phase data. The unwrapping procedure consists of finding the correct field number for each phase measurement [10–13].

The modulation phase Ψ obtained by unwrapping physically represents the fractional fringe order numbers in the Moiré images. The shape can be determined by applying the out-of-plane equation for Shadow Moiré:

$$Z(x, y) = \frac{p \left(\frac{\Psi(x, y)}{2\pi} \right)}{(\tan \alpha + \tan \beta)}, \quad (39)$$

where: $Z(x, y)$ = elevation difference between two points located on the body surface to be analyzed; p = frame period; α = light angle; β = observation angle.

The experiments are carried out using square wave grating with 1 mm frame grid period, light source is common white of 300 watts without using plane waves, light angle (α) and observation angle (β) are 45 degrees, the object surface is white and smooth and the resolution of photo is one megapixel. The phase stepping is made by displacing the grid in the horizontal direction in fractions of millimeters (Fig. 5).

To test the new equations for phase calculation, they were used with the technique of Shadow Moiré [13] for an object with known dimensions and to evaluate the error median by Eq. (40). This process was started with four images, repeated with five, then six and so on. The idea was to show that with increasing number of images the average error tends to decrease. Fig. 6 shows this procedure.

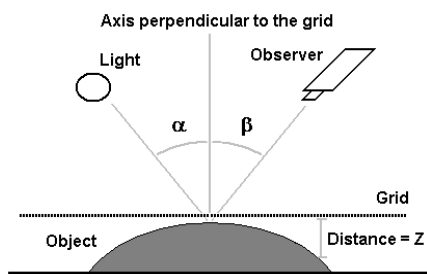


Fig. 5. Layout of experiment.

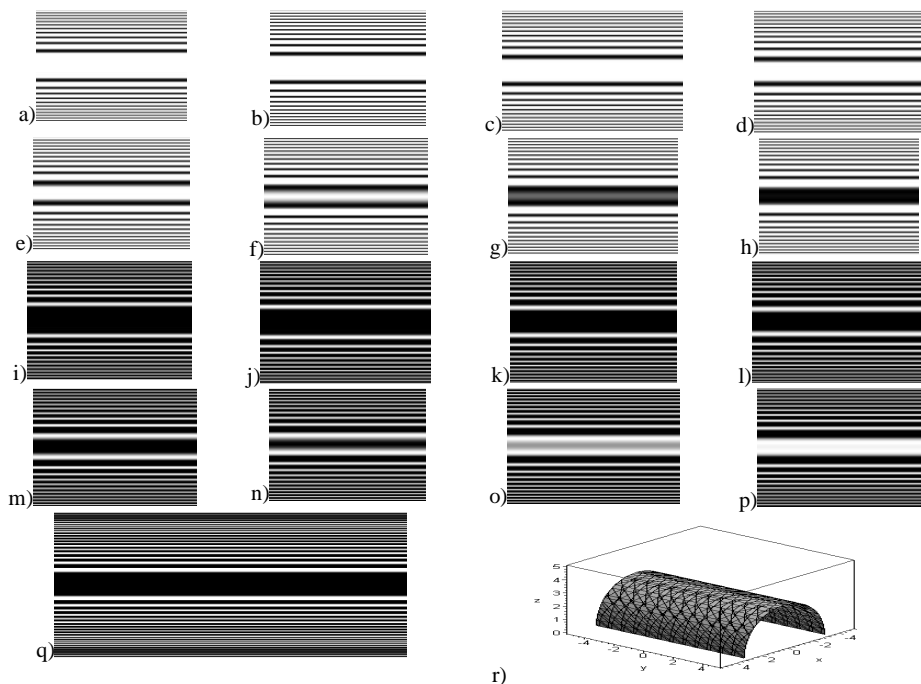


Fig. 6. One set of photos of 1 Megabyte (with low pass filter and Gaussian filter). Original Shadow Moiré images. 16-frame phase-shifting algorithm a–p. Wrapped phase q. Result in 3D r. (Semi-cylinder of a motor with diameter 6 cm, length 12 cm and with frame period of grid equals to 1 mm).

$$Error \quad Median \quad (E) = \frac{1}{M} \sum_{i=1}^M |Z_i^e - Z_i|, \quad (40)$$

where M is the number of pixels of the image, Z_i^e is the exact value of the size of the object being measured and Z_i is value measured by the new equation.

To compare the new equations for calculating the phase, 21 sets of 16 photos each were selected. Each set was computed using the average error of 4 to 16 images and using equations to evaluate the number of images. An average of errors was estimated, then 21 sets were evaluated using 4 to 16 images in each set ($\mu_4, \mu_5, \mu_6, \dots, \mu_{16}$). The hypothesis of testing on the difference in the means $\mu_A - \mu_B$ of two normal populations is being considered at the moment. A more powerful experimental procedure is to collect the data in pairs – that is, to make two hardness readings on each specimen, one with each tip. The test procedure would

then consist of analyzing the differences between the hardness readings on each specimen. If there is no difference between tips, the mean of the differences should be zero. This test procedure is called the paired t-test [14]. Specifically, testing $H_0: \mu_A - \mu_B = 0$ against $H_1: \mu_A - \mu_B \neq 0$. Test statistics is $t_0 = D / (S_D / \sqrt{21})$ where D is the sample average of the differences and S_D is the sample standard deviation of these differences. The rejection region is $t_0 > t_{\alpha/2, 20}$ or $t_0 < -t_{\alpha/2, 20}$. The data are shown below in Table 2.

Table 2. Error median error in μm versus number of frames (N) for a semi-cylinder with diameter of 6 cm and length of 12 cm (frame period of grid with 1 mm). It used 21 different sets of 16 images of Shadow Moiré (Fig. 6).

Error Median (μm)	Sets of Images																				
	Number of Images	1	2	3	4	5	6	7	8	9	10	11	12	13	14	15	16	17	18	19	20
4	125	127	125	128	129	128	126	125	128	127	127	127	129	127	127	127	127	127	126	126	127
5	121	122	122	123	123	124	123	123	124	121	122	121	123	124	122	124	125	122	121	123	121
6	118	118	118	119	120	120	119	120	120	120	121	119	119	117	117	118	121	118	119	121	119
7	113	113	116	117	115	113	116	113	115	115	113	116	115	113	115	116	116	113	113	116	114
8	109	110	111	110	110	111	111	109	112	110	111	112	109	112	110	111	111	112	112	110	110
9	107	105	107	106	106	107	106	107	105	107	104	107	106	108	104	107	104	104	105	105	105
10	103	104	103	102	104	103	102	101	102	102	104	103	103	102	100	101	104	100	103	101	100
11	99	100	98	99	98	100	97	96	98	98	100	100	98	98	99	99	99	99	99	96	100
12	94	94	95	93	92	93	95	95	95	96	95	95	95	92	93	93	92	93	92	95	92
13	89	89	91	88	90	89	90	88	92	91	90	88	88	88	91	88	88	89	90	89	89
14	84	84	87	87	85	87	85	86	86	87	84	87	86	87	84	84	85	87	85	84	87
15	82	81	83	84	81	81	85	83	83	85	82	83	85	81	83	82	85	85	84	85	83
16	79	81	78	77	78	78	78	81	80	78	79	79	78	80	80	80	78	78	77	81	78

Table 3. Testing hypotheses about the difference between two means with paired t-test, $H_0: \mu_A - \mu_B = 0$ against $H_1: \mu_A - \mu_B \neq 0$. The P -value is the smallest level of significance that would lead to rejection of the null hypothesis H_0 with the given data.

P-Value	Number of Images														
	N = 4	N = 5	N = 6	N = 7	N = 8	N = 9	N = 10	N = 11	N = 12	N = 13	N = 14	N = 15			
N = 4															
N = 5	0%														
N = 6	0%	0%													
N = 7	0%	0%	0%												
N = 8	0%	0%	0%	0%											
N = 9	0%	0%	0%	0%	0%										
N = 10	0%	0%	0%	0%	0%	0%									
N = 11	0%	0%	0%	0%	0%	0%	0%								
N = 12	0%	0%	0%	0%	0%	0%	0%	0%							
N = 13	0%	0%	0%	0%	0%	0%	0%	0%	0%						
N = 14	0%	0%	0%	0%	0%	0%	0%	0%	0%	0%					
N = 15	0%	0%	0%	0%	0%	0%	0%	0%	0%	0%	0%				
N = 16	0%	0%	0%	0%	0%	0%	0%	0%	0%	0%	0%	0%			

On performing the statistical test ($H_0: \mu_A - \mu_B = 0$ against $H_1: \mu_A - \mu_B \neq 0$) it was noticed that one cannot reject the zero hypothesis when using different equations with the same number of images. Also, the null hypothesis can be rejected when using different equations with different number of images with level of significance ($\alpha=0.05$). It was concluded that the

equations for phase calculation with a greater number of images are more accurate than those with a smaller number of images. The tests are shown in Table 3.

10. Conclusion

This paper deals with the equations for phase calculation in measurement with images method using the phase shifting technique. It describes several multistep phase shifting equations with the constant, but unknown phase step between the captured intensity frames. The new equations are shown to be capable of processing the optical signal of Moiré images. These techniques are very precise, easy to use and inexpensive. The results show that new equations are precise and accurate. On the basis of the performed error analysis it can be concluded that the new equations are very good phase calculation algorithms. These equations also seem to be very accurate and stable phase shifting algorithms with the unknown phase step for a wide range of phase step values. The metric analysis of the considered system demonstrated that its uncertainties of measurement depend on the frame period of the grid, on the resolution of photos in pixel and on the number of frames. However, the uncertainties of measurement of the geometric parameters and the phase still require attention. In theory, if we have many frames, the measurement errors will be very small. The measurement results obtained by the optical system demonstrate its industrial and engineering applications in experimental mechanics.

Acknowledgment

The authors thank the generous support of the Pontificia Universidade Catolica de Minas Gerais – PUCMINAS, as well as of the Conselho Nacional de Desenvolvimento Cientifico e Tecnológico – CNPq – “National Counsel of Technological and Scientific Development”.

References

- [1] H. Schreiber, J.H. Bruning: *Phase shifting interferometry*. D. Malacara (Ed.), Optical Shop Testing, Wiley Interscience, New York, 2007.
- [2] D. Malacara, M. Servín, Z. Malacara: *Interferogram Analysis for Optical Testing*. Taylor & Francis, New York, 2005.
- [3] K. Creath: “Phase-measurement interferometry techniques”. *Progress in Optics*, Elsevier Science Publishers, Amsterdam 1988, vol. 17, no.1 pp. 349–362.
- [4] J. Novak: “Five-step phase-shifting algorithms with unknown values of phase shift”. *International Journal for Light and Electron Optics*, 2003, vol. 114, no. 2, pp. 63–68.
- [5] J. Novak, P. Novak, A. Miks: “Multi-step phase-shifting algorithms insensitive to linear phase shift errors”. *Optics Communications*, 2008, vol. 281 no. 21. pp. 5302–5309.
- [6] P.S. Huang, H. Guo: “Phase-shifting Shadow Moiré Using the Carré Algorithm”. *Proceedings of the SPIE*, 2008, vol. 7066, no.1, pp. 70660B-70660B-7.
- [7] D. Malacara (ed.): *Optical shop testing*. John Wiley and Sons, New York 1992.
- [8] R.R. Cordero, J. Molimard, A. Martinez, F. Labbe: “Uncertainty analysis of temporal phase-stepping algorithms for interferometry”. *Optics Communications*, 2007, vol. 275, no. 1, pp. 144–155.
- [9] F.S. Hillier, G.J. Lieberman: *Introduction to operations research*. 8th. ed. [S.l.]: McGraw-Hill; New York 2005.
- [10] D.C. Ghiglia, M.D. Pritt: *Two-dimensional phase unwrapping: Theory, algorithms and software*. John Wiley & Sons, Inc., New York 1998.
- [11] J.M. Huntley: “Noise immune phase unwrapping algorithm”. *Appl. Opt.*, 1989, vol.28, no.1, pp. 3268–3270.

- [12]E. Zappa, G. Busca: “Comparison of eight unwrapping algorithms applied to Fourier-transform profilometry”. *Optics and Lasers in Engineering*, 2008, vol. 46, no. 2, pp. 106–116.
- [13]C. Han, B. Han: “Error analysis of the phase-shifting technique when applied to shadow moire”. *Appl. Opt.*, 2006, vol. 45, no.1, pp. 1124–1133.
- [14]M.F. Triola: *Elementary Statistics*. 10th. ed. Addison Wesley, Boston 2007.